CORNERING AERODYNAMICS ANALYSIS: 2023 CMR FSAE

Patrick Kozlowski, Brian Check, Balaji Sridhar
pkozlows, bcheck, bpsridha

ABSTRACT

This report compares the aerodynamic performance of Carnegie Mellon Racing's FSAE race car when it is driving straight to when it is turning. The study involved measuring the car's downforce and drag at varying speeds under both straight-line and cornering flow cases. The results of the study show that the aerodynamic package designed for the car is effective, generating downforce and drag forces that increase with increasing speed. Additionally, the cornering case resulted in a 2-3% reduction in performance, with the overall downforce to drag ratio being decreased. Overall, the study validates the effectiveness of CMR's aerodynamic package in generating downforce under various driving conditions, which is essential to understand to increase the car's cornering ability and overall performance.

INTRODUCTION AND BACKGROUND

Carnegie Mellon Racing, a student organization at Carnegie Mellon University, has a longstanding tradition of designing and building a formula 1-style electric race car every year to compete in FSAE competitions. The team's success in these competitions has been due to the critical components of the car, one of which is the aerodynamic package, specifically the front and rear wings. These wings are designed to generate downforce to help the car corner faster, which is critical in a race.

While extensive simulations have been conducted analyzing the car's performance when driving straight, the team has yet to study its performance throughout a turn. This is a crucial aspect of the race in which downforce generation is of utmost importance, and understanding, analyzing, and improving the downforce generation of the car throughout the entirety of a turn would significantly improve the performance of the car.

The goal of the project is to understand the car's aerodynamic "sensitivity" to turning air flow, meaning the reduction of downforce as a result of turning. By understanding the car's sensitivity to turning air flow, the team can optimize its performance by making necessary modifications to its design and setup.

For F1 teams, understanding how geometric properties of the car relate to aerodynamic properties is critical to creating a predictable, fast car. In addition to ensuring enough downforce is maintained, effective aero maps, which map aerodynamic performance to various car configurations, can also ensure the center of pressure of the car remains centralized so that the car does not oversteer or understeer under uncertain conditions [“What is Aero Mapping?”].

At the formula student level, judges have also repeatedly stated that analyzing aerodynamic performance under different conditions is critical to justifying aero's usefulness. Since FSAE cars typically experience high yaw angles, good straight-line numbers will not always result in better cornering [“Adding Aero”].

There are many approaches to understanding the sensitivity of an aero package, one of which is a technique known as “aero mapping”. Aero mapping is a complex tool used by racecar engineers to predict the behavior of a car to different set-up changes. These setup changes can include pitch angle, yaw angle, and roll angle of the car, each of which is visualized below. These changes and angles result from braking, acceleration, and turning of the car throughout the course of a race [“Tech Explained”].

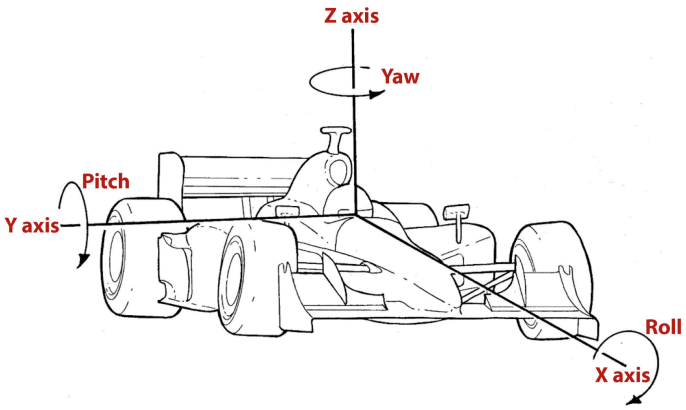

Figure 1: Roll, pitch, and yaw motions of a race car ["Racecar Vehicle Dynamics explained"]

One example of such a project is Monash motorsport, which independently analyzed each of these parameters. In their project, they examined how downforce and drag changed with yaw angle, roll angle, and front and rear ride heights (setting different front and rear ride heights is an alternative way of analyzing pitch angle). Their results found performance worsened as roll and yaw angle were increased, while performance peaked at certain pitch values. While their methodology was thorough and comprehensive, their simulations were all run under straight-line flow conditions, rather than simulating air with angular velocity relative to the car [Hendy].

Cal Poly's FSAE team took a different approach, simulating air turning with angular velocity relative to the car. They found between 3-7% reductions in downforce for corners of different radii, although they did not analyze the car under different roll/pitch conditions [Cal Poly].

This project initially aimed to combine the two approaches of Cal Poly and Monash by analyzing the car under different roll, pitch, and yaw conditions while using turning flow. This would give a complete picture, as accurate as possible, for Carnegie Mellon's car which could be used to assess the effectiveness of aerodynamic designs. However, due to difficulties encountered which led to less usable work time, it was decided to descope and only study the effect of turning flow on performance, rather than additionally analyzing roll, yaw, and pitch.

It is worth noting that while there have been many attempts at analyzing the aerodynamic sensitivity of formula-style vehicles, this project specifically addresses the unique challenges that come from the geometry of Carnegie Mellon's race car. Through this project, the goal is to contribute to the body of knowledge in the field of aerodynamics and racecar engineering, while also improving the performance and understanding of CMR's race car.

The report will first introduce the problem setup, including the domains used, mesh properties, and boundary conditions. The numerical formulation of the simulation will then be presented, addressing the methods and solvers used, and how these choices are beneficial or ideal for the problem. The results for each simulation are presented, with comparisons made when applicable and discussions provided. The report concludes with a summary of the project and final conclusions are made.

PROBLEM SETUP

The problem setup begins with implementing a simplified CAD model for the FSAE car. The model used, seen in Figure 3, consists of many of the main car components, including the wheels, chassis, driver upper body, headrest, front control arms, roll cage, hub motors, and front and rear wings. Compared to the full car image shown in Figure 2, it can be seen that the model is a fairly accurate representation, and many of the components not included were deemed not as important to the overall car aerodynamics, either because they are too small to make a large difference, such as the suspension or wing attachment arms, or because there is another component that will likely cause the component in question to be unnecessary, such as not including rear wheel control arms because front wheel arms will cause flow to be distorted at back arm locations.

Figure 2: CMR 2023 FSAE Car

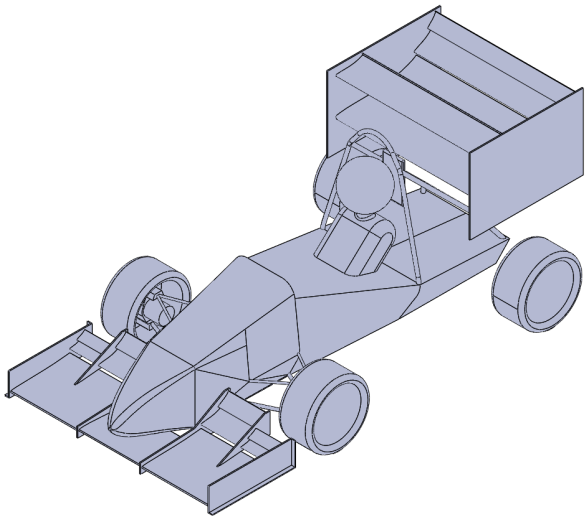

Figure 3: Simplified CAD model

With the CAD model ready for implementation, the boundary conditions for both straight-line and corner domain are decided. Both domains have identical wall conditions and outlet specifics, with only the flow and ground movement directions changing between scenarios. Table 1 shows the details of each wall or zone boundary conditions.

Table 1: Boundary Conditions

Boundary	Condition
Car	Wall: No Slip, Stationary
Ground	Wall: No Slip, Moving
Domain Exterior	Wall: Free Shear, Stationary
Car Wheels	Wall: No Slip, Rotating
Wheel Radii	Wall: Free Shear, Stationary
Inlet	Velocity: Magnitude/Direction Turbulence: Intensity = 0.5% Viscosity Ratio = 2.0
Outlet	0 Gauge Pressure Turbulence: Intensity = 0.5% Viscosity Ratio = 2.0

As seen in Table 1, the majority of the stationary walls on the interior of the domain are no-slip walls, with the exception of the Wheel Radii faces, which connect the moving Ground to the rotating Car Wheels. These are set to free-shear walls, similar to the external walls and ceilings of both domains. Each moving wall is a no-slip wall. The inlet and outlet specifications are discussed in more detail in the following domain setup sub-sections.

Straight-Line Domain Setup

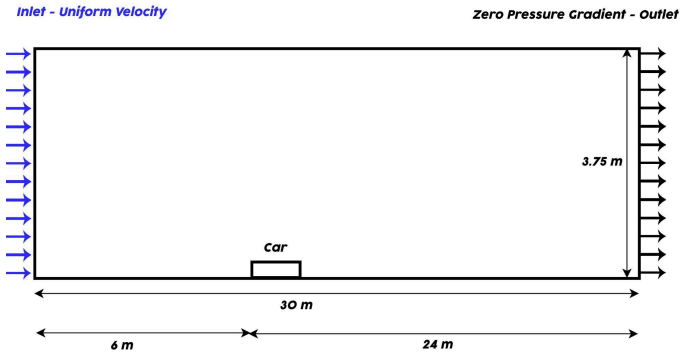

Figure 4: Straight-line Domain: Top view

In the context of simulating a behavior of the car in a straight-line, a domain with a width of 3.75 m, a length of 30 m, and a height of 6 m is considered. Due to symmetry, only half of the car is taken into account in the simulation. The car is placed 6 m away from the inlet, which is characterized by varying velocity conditions of 10m/s, 15 m/s, 20 m/s, and 30 m/s. The purpose of this variation is to analyze the effect of the car's speed on the simulation results. The ground is assumed to be a no-slip surface with the same velocity as the inlet condition.

To replicate the motion of the car, which is moving in real-life scenarios, the ground is set to move in the direction of the inlet velocity, and at the same velocity as the inlet. In this study, the rotational movement of the car wheels was taken into account to simulate a more realistic scenario. The angular velocity of the wheels was calculated based on the velocity of the inlet flow, and the values used in the simulations were 87.489 rad/s for a flow velocity of 20 m/s, 43.779 rad/s for 10 m/s, 65.61675 rad/s for 15 m/s, and 131.2335 rad/s for 30 m/s. By incorporating the rotational movement of the wheels, the simulation results are expected to more accurately reflect the actual behavior of the car in motion.

Corner Domain Setup

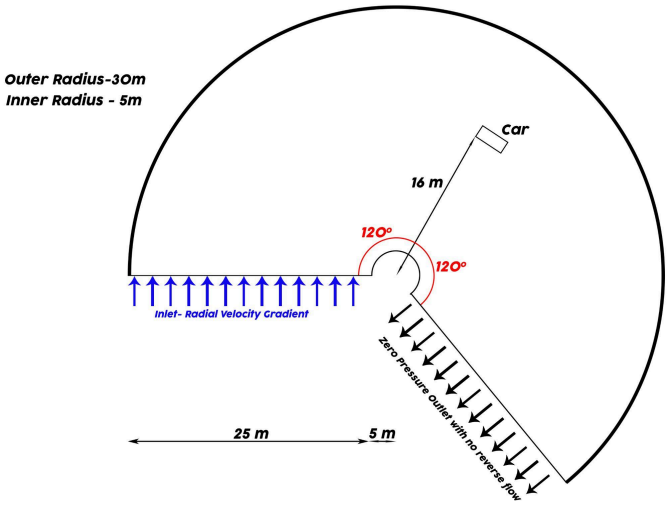

Figure 5: Corner Domain: Top view

In the context of simulating the behavior of a car in a cornering domain, a pie-shaped domain with an outer radius of 30 m and an inner radius of 5 m, covering 240o is considered. To capture the varying inlet velocity gradient, the inlet velocity is defined with a radial velocity and a directional component. As the aerodynamic effect on the car is not symmetrical, the entire car is added to the domain. The car is positioned 16 m away from the rotational axis and equidistant between the inlet and outlets. The outlet is defined as a zero-pressure gradient outlet.

The simulation is performed for different velocities ranging from 10m/s, 15 m/s, 20 m/s, and 30 m/s, affecting the inner wheel of the car. The purpose of this variation is to analyze the influence of the car's speed on the simulation results. To mimic the car's motion in real-life scenarios, the ground is set to move in the direction of the inlet velocity and at the same velocity as the inlet. Similar to the straight-line case, in the cornering mesh the rotational movement of the car wheels was taken into account to simulate a more realistic scenario. The angular velocity of the wheels was calculated based on the velocity of the inlet flow, and the values used in the simulations were 87.489 rad/s for a flow velocity of 20 m/s, 43.779 rad/s for 10 m/s, 131.234 rad/s for 15 m/s, and 262.467 rad/s for 30 m/s.

Meshing

The Ansys Fluent Watertight Geometry Meshing Workflow was used to generate the mesh for both domains. Sizing specifics applicable to both domains can be found in Table 2.

Table 2: Mesh Specifics

Region	Minimum Cell Size
Surface: Near-field	16 mm
Surface: Mid-field	64 mm
Surface: Far-field	256 mm
Volume: Near-field	16 mm
Volume: Mid-field	64 mm
Volume: Far-field	512 mm
Boundary Layer: Δy	0.5 mm
Boundary Layer: Δy^+	30

In addition to the various refinement regions for the car and wake regions, multiple curvature refinement regions were implemented on multiple car components for the surface mesh. These include small sizings for the front and rear wings, as well as additional refinements for the chassis, wheels, and wheel radii. This allowed the car model to be accurately represented in the mesh and the volume mesh to be generated without areas of concern. The volume mesh was generated using poly-hexcore cells, which implement tetra-cells in regions of consistent sizings, and poly-cells where these regions meet.

The straight-line domain mesh can be seen in Figure 6, with each refinement area visible. Similarly, Figure 7 shows the corner domain along with refinement regions. The mesh sizings (Table 2) are consistent across both domains.

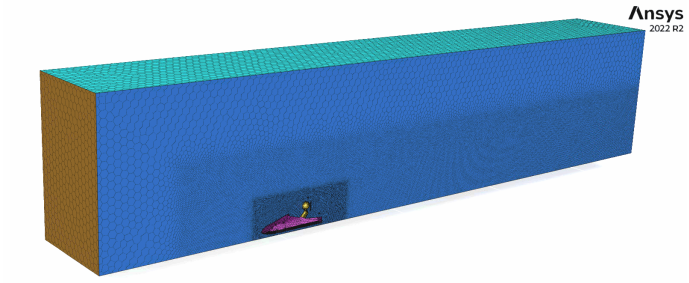

Figure 6: Straight-line Domain / Mesh

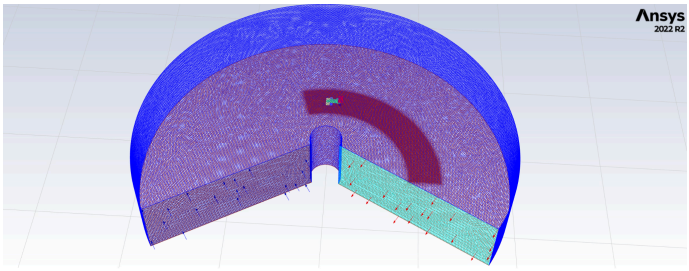

Figure 7: Corner Domain / Mesh

Figure 8 shows a cut-plane view of the near-field

volume mesh along with the meshing around the car. Darkened areas on the wings and chassis show the curvature refinements that allowed for increased model accuracy. Figure 9 shows a close up of the boundary layer mesh found along the car faces. This layer consists of 10 layers of cells, starting from an initial height of 0.5 mm and increasing in height at a rate of 20%. This sizing was determined based on the flow speed and car size, resulting in an estimated Reynold's number of 4,000,000 and a Δy^+ of 30. These tetra-cells are needed for better boundary-layer flow convergence, and will ideally improve the accuracy of flow movements around the car.

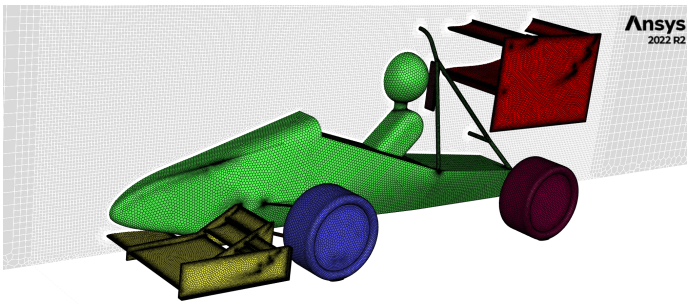

Figure 8: Car / Near-Field Mesh

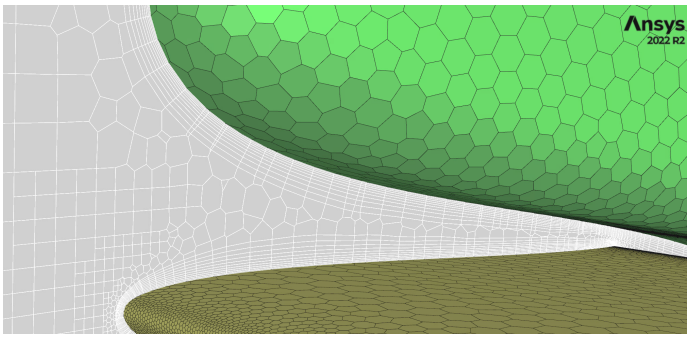

Figure 9: Car, Boundary-Layer Mesh

Both meshes had a resulting minimum orthogonality component of above 0.1, which is the recommended minimum value for an ideal mesh. The final straight-line mesh consisted of 8 million cells, and the final corner domain consisted of 21 million cells.

NUMERICAL FORMULATION

The numerical formulation to be presented applies to both straight-line and corner simulations.

The flow being modeled in both simulations is assumed to be incompressible, and the steady-state pressure based solver is used. Based on the average flow velocity and car length, the estimated Reynold's number for the flow is around 4,000,000. Due to this expected turbulence and importance of the boundary-layer flow in the system, the RANS k-ω shear-stress transport (SST) model was chosen. The solution method used was the pressure-velocity coupled scheme. For discretization schemes, see Table 3. The benefits of the turbulence model and numerical solver are outlined below.

ANSYS k-ω SST Turbulence Model: The purpose of the k-ω SST turbulence model is to effectively blend the accurate formulation of the k-ω model in the near-wall region with the freestream independence of the k-ϵ model in the far field. The k-ω SST model is similar to the standard k-ω model, but includes the following refinements [Ref. 1]:

- The standard k-ω and the transformed k-ϵ models are multiplied by a blending function and added together. The blending function is designed to be one in the near-wall region (activates the standard k-ω model) and zero away from the surface (activates the transformed k-ϵ model).
- The SST model incorporates a damped cross-diffusion derivative term in the ω equation.
- The definition of the turbulent viscosity is modified to account for the transport of the turbulent shear stress.
- The modeling constants are different.

ANSYS Coupled algorithm: The coupled algorithm solves the momentum and pressure-based continuity equations together. The full implicit coupling is achieved through an implicit discretization of pressure gradient terms in the momentum equations, and an implicit discretization of the face mass flux, including the Rhie-Chow pressure dissipation terms. The coupled scheme obtains an efficient single-phase implementation for steady-state flows, with increased performance when compared to the segregated pressure-velocity coupled solution schemes [Ref. 2].

Table 3: Spatial Discretizations

Variable	Discretization Scheme
Gradient	Least Squares Cell Based
Pressure	Second Order
Momentum	Second Order Upwind
Turbulent Kinetic Energy	Second Order Upwind
Specific Dissipation Rate	Second Order Upwind

The Second Order Upwind discretization method for momentum, turbulent kinetic energy, and specific dissipation rate is described below.

ANSYS Second-Order Upwind Scheme: Quantities at cell faces are computed using a multidimensional linear reconstruction approach. In this approach, higher-order accuracy is achieved at cell faces through a Taylor series expansion of the cell-centered solution about the cell centroid. When second-order upwinding is selected, the face value is

computed using the following expression:

$$\phi_{f,SOU} = \phi + \nabla\phi * \vec{r} \quad (1)$$

In Equation 1, ϕ is the cell-centered value and $\vec{r}$ is the displacement vector from the upstream cell centroid to the face centroid [Ref. 3].

RESULTS AND DISCUSSION SECTION

Straight-line Results and Discussion

The initial straight-line simulations were completed to get a better understanding of the downforce and drag production for the car, confirm accuracy of results for the proposed solvers and models, and to get a baseline for comparison of the cornering simulation results. As mentioned in the Problem Setup section, the first straight-line simulations were run at 20 m/s using three different setups regarding the car's aerodynamic package. These setups include a no aero package (no front or rear wing) for a baseline reading and two setups with different rear-wing configurations. These rear-wing changes are a result of the Drag-Reduction System (DRS) implemented on the wing, allowing the driver to configure the rear wing based on desired outputs: decreased drag for straight-line (DRS active) and increased downforce for corners (DRS inactive). In terms of force outputs, this system should ideally result in significantly higher downforce when DRS is inactive, and significantly lower drag when DRS is active.

The resulting scaled residual plots for the full aero (DRS inactive) and no aero configurations are shown in Figures 10, 11.

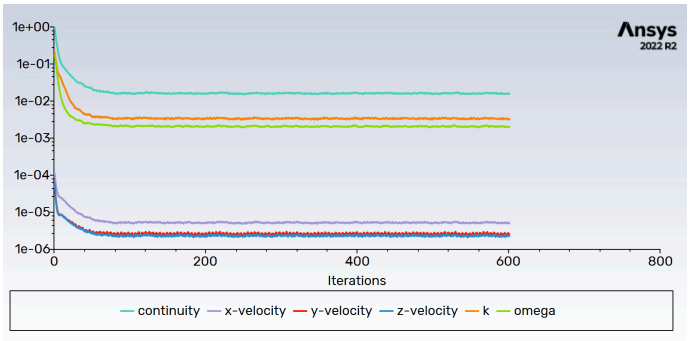

Figure 10: Straight-line Scaled Residuals: No-Aero

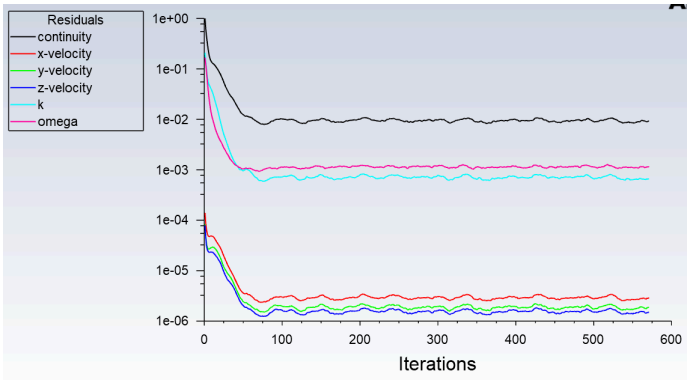

Figure 11: Straight-line Scaled Residuals: Full Aero

These scaled residual plots showed acceptable levels of convergence, confirming the numerical schemes and solvers used were effective. This allows future simulations to be run using the same mesh characteristics and solver processes, knowing convergence will likely be reached.

The simulations produced the following results for downforce and drag for each configuration:

Table 4: Straight-line Simulation Results (20 m/s)

No Aero Package	Value
Downforce (N)	-47.1
Drag (N)	117.4
Downforce:Drag Ratio	-0.401
Aero Package: DRS Active	**Value**
Downforce (N)	415.64
Drag (N)	231.57
Downforce:Drag Ratio	1.795
Aero Package: DRS Inactive	**Value**
Downforce (N)	598.9
Drag (N)	348.1
Downforce:Drag Ratio	1.721

The results in Table 4 highlight the effectiveness of the aero packages in generating downforce for the car, following expected behavior. The baseline model of the car has a net vertical lift component of 47.1 N with drag force of 117 N, resulting in a downforce:drag ratio of -0.401. The upward lift generated in this portion is certainly detrimental to the car's cornering capability as the tires will lose traction and begin to slip much more quickly.

Adding the full aero package, consisting of front and rear wings, increased the net downforce by 646 N while also increasing the drag due to the increase of surface area of the car. This results in a downforce:drag ratio of 1.721. Because

drag is typically not a limiting factor on a turn, but rather the ability of the tires to maintain grip due to lateral acceleration, the drastic increase in downforce is very beneficial to the car's performance even at the expense of higher drag.

Lastly, the Drag Reduction System is shown to be very effective, as it reduces the net drag on the car by 33% when compared with DRS Inactive. This means that when the car is on a straight and needs to accelerate, DRS can be activated and will be effective in enhancing the performance of the car.

Additionally, the pressure contours and pathlines for each simulation are examined to confirm expected behavior as well as examine which areas of the aero package are most impactful. The pressure contours at the midplane of the car along with streamlines of the car are shown below.

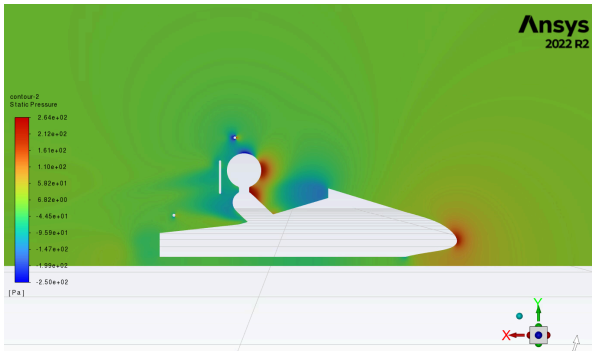

Figure 12: Straight-line Pressure Contour: No-Aero

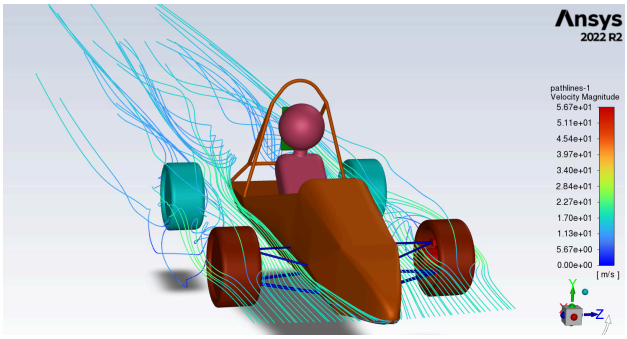

Figure 13: Straight-line Pathlines: No-Aero

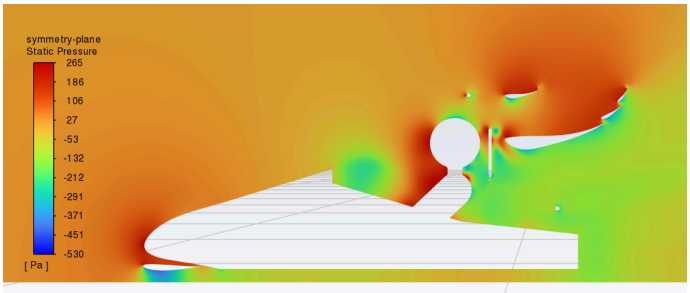

Figure 14: Straight-Line Pressure Contour: Full Aero

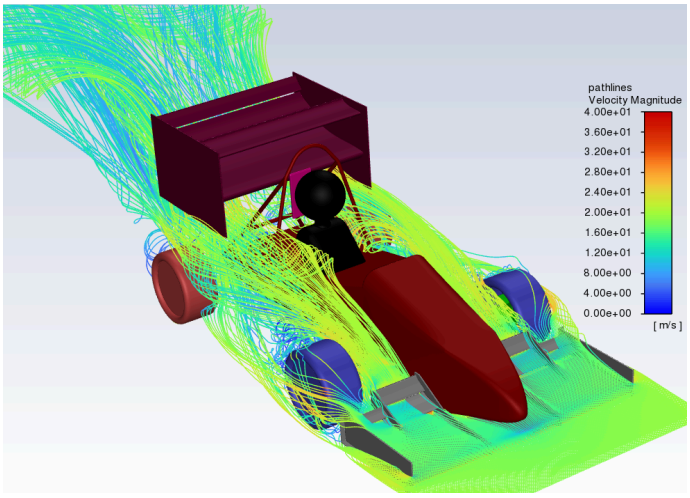

Figure 15: Straight-line Pathlines: Full Aero

In both cases, the pathlines seem to follow expected behavior. In the no aero case, they flow around the chassis and wheels as expected, with increased turbulence behind the spinning wheels and chassis. In the full aero case, the air is initially laminar and is directed upwards by the front wing. As it flows around the wheels and chassis, a large turbulent wake is developed behind the car and wheels.

As seen in Figure 12, there are high pressure regions in front of the car and driver, with low pressure regions behind them. This pressure differential explains the drag on the car. Additionally, the pressure above and below the car is relatively even, explaining why the overall lift is very low. Positive lift was likely generated by the spinning wheels and possibly slightly due to the chassis shape.

As seen in Figure 15, the full aero package has high pressure on top of the front and rear wings, with low pressure below them. This pressure differential is what causes downforce on the car and follows expected behavior. A directional component of the high pressure on top of the wing also acts backward, as the wings are angled upwards; this explains the increased drag on the car when aero is added. Additionally, the extreme pressure differential on the rear wing caused by the second and third elements explains why there is such a drastic decrease in drag when DRS is activated.

The next set of straight-line simulations are run using just one of the aerodynamics package setups (DRS inactive) at 4 different speeds: 10, 15, 20, and 30 m/s. These results will be used to compare the forces produced in the corner cases, as the rear wing setups are the same.

Table 5: Straight-line Simulation Results (DRS Inactive)

10 m/s	Value
Downforce (N)	142.64
Drag (N)	84.012
Downforce:Drag Ratio	1.697
15 m/s	**Value**
Downforce (N)	331.56
Drag (N)	194.62
Downforce:Drag Ratio	1.703
20 m/s	**Value**
Downforce (N)	598.9
Drag (N)	348.1
Downforce:Drag Ratio	1.721
30 m/s	**Value**
Downforce (N)	1371.4
Drag (N)	786.66
Downforce:Drag Ratio	1.743

The downforce:drag ratio seems to increase slightly with higher velocities, but overall remains relatively consistent at around 1.7-1.75. The closeness of the values indicates that results from 20 m/s simulations can be extrapolated and applied at different speeds, as the aero package is still effective. This is significant as it confirms the design and analysis of the car in the future can be performed at one speed, rather than at many while still being effective. The increased ratio at higher velocities may be due to faster, more turbulent air under the wing causing improved flow attachment. Another possible explanation is that the effect of spinning wheels becomes less significant when faster air is already more turbulent.

Cornering Results and Discussion

In this study, an analysis was conducted of the cornering case to investigate the downward force exerted on a car while turning. The initial assumption was that during the cornering case, there would be a reduction in downforce on the car due to a decrease in the surface area of the wings that interact perpendicularly with the air flow.

In order to ensure the accuracy and reliability of the simulation results, it is crucial to verify the convergence of the numerical schemes and solvers utilized. Figure 16 displays the residual plot, which serves as a measure of convergence by indicating the difference between successive iterations in the solution process. In this case, the plot shows acceptable levels of convergence, which confirms the effectiveness of the chosen numerical schemes and solvers. This provides a strong basis for future simulations to be run using the same mesh characteristics and solver processes, with confidence that convergence will likely be reached.

Figure 17 was analyzed to observe the velocity magnitude contour specifically from the 20m/s cornering case. The contour clearly shows that the velocity is not uniformly flowing along the car, but instead has an initial gradient that changes as it flows through the domain. The inner wheel of the car experiences a velocity of 20 m/s in this particular plot, which is consistent with the expected values during the problem formulation. Additionally, the contour allows for observation of the velocity gradient profile behind the car. The profile provides further evidence that the velocity being experienced by the car in the simulation is consistent with expectations. Similar results were observed in the other velocity cases with the respective velocities at the inner wheel of the car. It can be noted that the car experiences slightly higher velocity than expected at the inner wheel due to the gradient nature of the velocity.

Figure 18 shows the flow of pathlines around the car from the front view in the 20m/s cornering case. The curvature of the flow can be observed, which confirms the expected behavior of the flow around the car. Additionally, the formation of turbulence around the front wing and in the wake region is also observed, which is consistent with the anticipated flow pattern. However, it should be noted that the curvature of the flow might not appear greater than it might seem because the radius of turn in the simulation was relatively large. Despite this, the observed flow pattern is consistent with the expected behavior and supports the accuracy of the simulation results.

In Figure 19 and 20, it can be observed that the pressure gradient distribution on the surface of the car, specifically from the 20 m/s cornering case. The pressure distribution helps in identifying the difference in pressure acting on the surface of the car, thereby highlighting the asymmetrical nature of the flow. Upon close observation, it can be seen that there is a slight difference in pressure being applied on the chassis region, with higher pressure being applied on the left side of the car than the right. Similarly, the pressure difference in the wings can be seen, with higher pressure being exerted on the side where the velocity hits the car and less on the inner side of the wing. This slight asymmetry in the pressure distribution was expected and provides support for the results in the forces generated in this particular case. By analyzing the pressure gradient on the surface of the car, a better understanding of the flow behavior and the forces acting on the car during cornering can be reached.

Figure 21 shows the pressure gradient around the car specifically from the 20 m/s cornering case. The pressure difference around the car will give an idea as to how the pressure difference around the car would be and in turn give information about the locations of where down force could be expected. In this figure it can clearly be seen that the wings are behaving as they were designed to behave by creating lower pressure under the wing which would lead to a downward force on the car. This phenomenon can be seen in both the front and back wings of the car. This shows that the forces being generated on the car can be relied upon for analysis and

comparison.

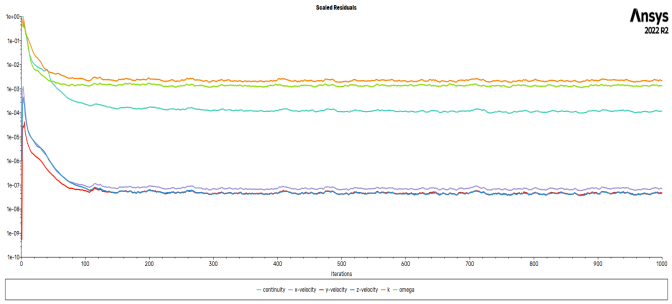

Figure 16: Residuals

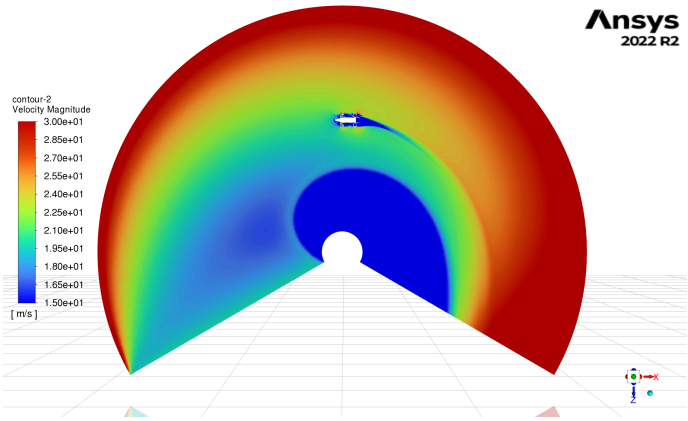

Figure 17: Velocity Magnitude Contour

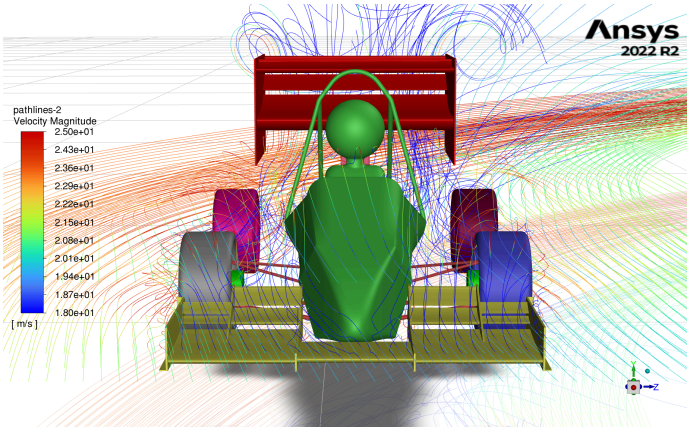

Figure 18: Pathlines around car: front view

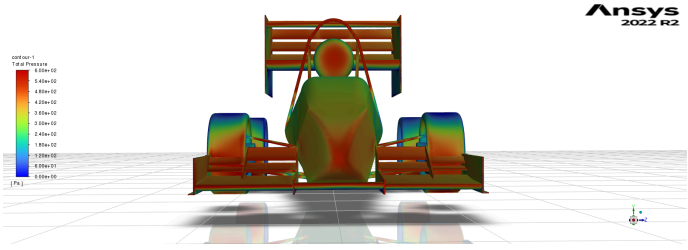

Figure 19: Pressure contour on the car: front view

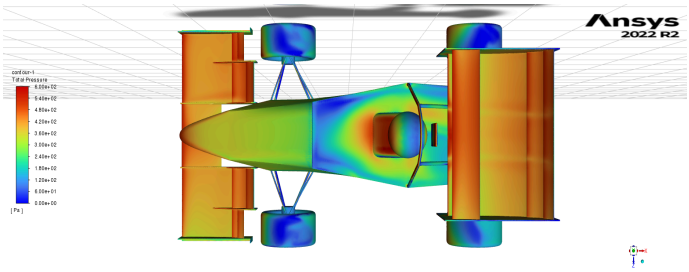

Figure 20: Pressure contour on the car : Top view

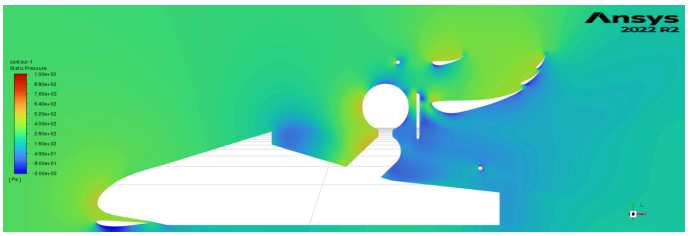

Figure 21: Pressure around the car

Table 6 displays the calculated values for downforce, drag, and the downforce-to-drag ratio at each of the four simulated speeds. These findings reveal that as the velocity increases, there is a corresponding increase in both the downforce and drag forces acting upon the car. Furthermore, the ratio of downforce to drag also shows a gradual increase from 1.630 to 1.701 with an increase in velocity.

These results suggest that at higher velocities, the car experiences greater aerodynamic forces, resulting in a higher downforce-to-drag ratio. This trend is consistent with the well-known fact that as the car's velocity increases, so does the importance of aerodynamics for vehicle performance. The increased downforce-to-drag ratio at higher velocities indicates that the car can generate more downforce per unit of drag, which is desirable for optimal vehicle handling and stability during high-speed maneuvers.

Table 6: Corner Simulation Results (DRS Inactive)

10+ m/s	Value
Downforce (N)	163
Drag (N)	100
Downforce:Drag Ratio	1.630
15+ m/s	Value

Downforce (N)	373
Drag (N)	225
Downforce:Drag Ratio	1.658
20+ m/s	Value
Downforce (N)	675
Drag (N)	404
Downforce:Drag Ratio	1.671
30+ m/s	Value
Downforce (N)	1556
Drag (N)	915
Downforce:Drag Ratio	1.701

Comparisons between Straight-line and Cornering Results

Before comparing Tables 5 and 6, a discrepancy requires addressing related to the labeled speeds in the straight-line and cornering cases. In the straight-line case, the labeled speeds remain constant over the width of the car, while in the cornering case, the speed across the width of the car is above the labeled values and increases by an estimated 2 m/s from inner to outer wheel, despite the speeds at the inner wheel matching the labeled values. This discrepancy introduces a level of complexity to the analysis, making direct comparisons of downforce and drag numbers less accurate indicators of the impact of cornering on aerodynamic performance.

However, even with this discrepancy, the data provides valuable insights into the effects of cornering on aerodynamic performance. Rather than comparing absolute numbers, a more effective method of comparison is to examine the ratio of downforce to drag. This approach is beneficial because the ratio of these two factors is not solely dependent upon the car's speed, but also considers the aerodynamic characteristics of the car's design.

In evaluating the impact of cornering on the car's aerodynamic performance, it is crucial to understand the significance of downforce and drag. Downforce is the vertical force that a car generates due to its design, which presses the tires into the road, improving the car's grip and handling during cornering. On the other hand, drag is the force that resists the car's motion, acting in the opposite direction of the car's movement, which is a critical factor in determining the car's top speed and acceleration.

By analyzing the downforce:drag ratio, one can draw important conclusions about the car's performance during cornering. For instance, if the ratio is high, it suggests that the car generates a significant amount of downforce relative to drag, which means that the car can maintain high speeds while navigating corners. Conversely, a low ratio indicates that the car generates more drag than downforce, which would impede its performance during cornering.

By comparing the Downforce:Drag ratios in Tables 5 and 6, it is clear that the car's overall performance decreases through a corner. For similar velocities, the ratio is higher in the straight-line case than in the corner case. This means that overall, the car appears to underperform as a whole in the cornering domain setup.

The overall reduction in downforce:drag ratio at each speed is for both straight line and cornering cases in Table 7 below.

Table 7: Straight Line vs. Cornering Downforce:Drag

Speed	Straight Line	Cornering	Percent Reduction
10+ m/s	1.697	1.630	2.45
15+ m/s	1.703	1.658	2.64
20+ m/s	1.721	1.671	2.91
30+ m/s	1.743	1.701	2.41

Table 7 demonstrates a consistent decrease in the downforce-to-drag ratio by 2-3 percent across all speeds. This decrease appears to be independent of the simulated velocity. This observation is reasonable, as each simulation was performed at a fixed radius, which should result in the flow following the same path and experiencing a similar decrease in downforce and increase in drag at each speed due to the angled interactions with the car's geometry.

This reduction in the downforce-to-drag ratio is a crucial consideration for high-performance vehicle design. While an increase in downforce is desirable for vehicle stability and handling, it comes at the cost of increased drag, which can reduce the car's top speed and fuel efficiency. The results suggest that for a given car design and corner radius, there may be an optimal speed range for maximizing the downforce-to-drag ratio.

The underlying physics of this phenomenon can be attributed to the fact that at higher speeds, the airflow over the vehicle's surface becomes more turbulent, leading to a decrease in the efficiency of the wing profiles in generating downforce. In contrast, the drag force increases due to the increased friction between the air and the car's surface.

Overall, these results show that while there is a reduction in performance of the aerodynamics during a turn, the aero package is still effective and should improve the performance of the car during a turn. A 2-3 percent reduction still leaves the car with vastly more downforce than if there was no aero on the car.

In conclusion, the comparison of cornering case and straight-line case reveals the car will underperform in cornering scenarios. Further research is needed to better understand the effects of rotating flow on car performance, and to develop more effective strategies for improving performance in corner cases. An additional takeaway from this project was the development of a domain setup and modeling technique which can be used by Carnegie Mellon Racing in future years to quickly analyze performance of their car throughout a turn when designing and analyzing new aerodynamic designs.

SUMMARY AND CONCLUSIONS

This project served as a means to demonstrate the importance of the aerodynamics package on a FSAE car. By implementing simulations in both a straight-line and cornering scenario at varying speeds, it was shown that the performance of the aerodynamic package is dependent on multiple factors, including the speed and direction of the air flow around the car. The project also shows the complexity of simulating a cornering vehicle, with many areas for assumptions or estimations that may lead to results that differ from the expected. The following conclusions can be drawn from the project:

- The implementation of an aerodynamic package, which included front and rear wings, was found to significantly increase the generated downforce for a given speed, while simultaneously increasing drag. This resulted in a marked improvement in the overall Downforce:Drag ratio.
- The simulation results showed that the downforce generated by the aerodynamic package increases with velocity in both straight-line and cornering scenarios. This suggests that higher speeds lead to a greater amount of downforce being generated.
- Applying a rotational velocity around the car did not have a large impact on the downforce generation, but did have a more significant impact on the drag from the car. The overall performance in terms of the Downforce:Drag ratio decreases when comparing straight-line vs. corner simulations for a given speed.
- 2-3% reduction in downforce:drag ratio was observed from the straight line case to the cornering case.

REFERENCES

1. Ansys® Academic Student Fluent, Release 22.2, Help System, Turbulence, ANSYS, Inc.
2. Ansys® Academic Student Fluent, Release 22.2, Help System, Pressure-Velocity Coupling, ANSYS, Inc.
3. Ansys® Academic Student Fluent, Release 22.2, Help System, Discretization, ANSYS, Inc.
4. Cal Poly. “Design and Fabrication of a Small UAV Using Carbon Fiber and Rapid Prototyping.” Cal Poly, 2010, https://digitalcommons.calpoly.edu/cgi/viewcontent.cgi?article=1156&context=aero_fac.
5. Hendy, Paul. "Aero Map for Formula Student." MMS Final Year Thesis Collection, 2019, https://static1.squarespace.com/static/5e2a78aea2dc434ac475b5a4/t/5f8cc8c05980767192e24c5c/1603061992342/MMS+Final+Year+Thesis+Collection+-+Aero+Map+for+Formula+Student+%28Paul+Hendy+-+2019%29.pdf.
6. "F1 Chronicle." What Is Aero Mapping in F1?, F1 Chronicle, 2021, https://f1chronicle.com/what-is-aero-mapping-in-f1/#:~:text=on%20the%20track.-,What%20is%20aero%20mapping%20in%20F1%3F,tuning%20capabilities%20to%20the%20aerodynamics.
7. F1 Chronicle. "What Is Aero Mapping in F1?" F1 Chronicle, 26 Jan. 2021, https://f1chronicle.com/what-is-aero-mapping-in-f1/#:~:text=on%20the%20track.-,What%20is%20aero%20mapping%20in%20F1%3F,tuning%20capabilities%20to%20the%20aerodynamics.
8. "Tech Explained." Racecar Engineering, https://www.racecar-engineering.com/tech-explained/what-is-an-aero-map/.
9. "Adding Aero: Justifying Aero." DesignJudges, https://www.designjudges.com/articles/adding-aero-justifying-aero.
10. “Aerodynamics of an FSAE Car” Ansys Innovation Spaces, https://courses.ansys.com/index.php/courses/aerodynamics-of-an-fsae-car/
11. “Racecar Vehicle Dynamics explained” https://www.racecar-engineering.com/tech-explained/racecar-vehicle-dynamics-explained/